

Da: em.crad.0.6c04f2.2d64eba6@editorialmanager.com

per conto di

Clinical Radiology <em@editorialmanager.com>

mer 17/06/2020 17:24

A: palmisano anna

Dear Dr Palmisano

Re: CLINICAL RADIOLOGY CRAD-D-19-00993R1: MRI prediction of pathological response in locally advanced rectal cancer: when ADC radiomics meets conventional volumetry

I am very pleased to tell you that your paper has been accepted for publication in Clinical Radiology.

It is being published on the understanding that the material has not been published elsewhere, the only permissible exception being if you refer to the earlier publication with a specific reference.

You will receive proofs from the publisher in due course, and they will be in touch regarding copyright. It is therefore important that we are notified of any e-mail address changes.

A few weeks after your article is published you will receive an e-mail request to complete a survey. Your feedback will help improve the quality of support offered to you and your colleagues, and we would really appreciate it if you could take the time to complete survey

Once again, congratulations and I do hope that you will consider sending further papers for possible publication in Clinical Radiology.

Best regards

Dr Michael Weston
Editor

=====

Clinical Radiology
The Royal College of Radiologists
63 Lincoln's Inn Fields
London
WC2A 3JW

Registered Charity No.: 211540

Clinical Radiology

MRI prediction of pathological response in locally advanced rectal cancer: when ADC radiomics meets conventional volumetry

--Manuscript Draft--

Manuscript Number:	CRAD-D-19-00993R1
Full Title:	MRI prediction of pathological response in locally advanced rectal cancer: when ADC radiomics meets conventional volumetry
Article Type:	Original Paper
Corresponding Author:	Anna Palmisano Ospedale San Raffaele Milan, ITALY
Corresponding Author Secondary Information:	
Corresponding Author's Institution:	Ospedale San Raffaele
Corresponding Author's Secondary Institution:	
First Author:	Anna Palmisano
First Author Secondary Information:	
Order of Authors:	Anna Palmisano Alessandra Di Chiara, MD Antonio Esposito, MD Paola Maria Vittoria Rancoita, PhD Claudio Fiorino, PhD Paolo Passoni, MD Luca Albarello, MD Riccardo Rosati, MD Alessandro Del Maschio, MD Francesco De Cobelli, MD.
Order of Authors Secondary Information:	
Abstract:	<p>Purpose: To investigate the role of DWI-images, T2w-images and ADC histogram analysis before, during and after neoadjuvant chemo-radiotherapy (CRT) in the prediction of pathological response in patients with locally advanced rectal cancer (LARC).</p> <p>Methods: 1.5T MRI was performed in 43 patients with LARC before, during and after CRT. Tumour volume was measured on both T2-weighted (V_{T2w}) and on DWI b_1000 images (V_{b_1000}) at each time point, hence tumour volume reduction rate (ΔV_{T2w} and ΔV_{b_1000}) was calculated. Whole lesion (3D) first order texture analysis of ADC map was performed. Imaging parameters were compared to pathological Tumour Regression Grade (TRG). The diagnostic performance of each parameter in the identification of complete responders (CR:TRG4), partial responders (PR:TRG3) and no responders (NR:TRG 0-2) was evaluated by multinomial regression analysis and receiver operating characteristics curves.</p> <p>Results: After surgery 11 patients resulted CR, 22 PR, 10 NR. Before CRT, predictor of CR resulted ADC 75° percentile and median, with good accuracy (74% and 86%, respectively) and sensitivity (73% and 82%, respectively). During CRT, best predictor</p>

of CR resulted ΔV T2w (-58.3%) with good accuracy (81%) and excellent sensitivity (91%). After CRT, best predictors of CR resulted ΔV T2w (-82.8%) and ΔV b,1000 (-86.8%), with 84% of accuracy in both cases and 82% and 91% of sensitivity, respectively.

Conclusions: Median ADC value at pre-treatment MRI and ΔV T2w (from pre-to-during CRT MRI) may have a role in early and accurate prediction of response to treatment. Both ΔV T2w and ΔV b,1000 (from pre-to-post CRT) help in the identification of CR after CRT.

MRI prediction of pathological response in locally advanced rectal cancer: when ADC radiomics meets conventional volumetry

Authors

Anna Palmisano¹ MD, Alessandra Di Chiara^{1,2} MD, Antonio Esposito^{1,2} MD, Paola Maria Vittoria Rancoita³ PhD, Claudio Fiorino⁶ PhD, Paolo Passoni⁴ MD, Luca Albarello⁵ MD, Riccardo Rosati^{2,7} MD, Alessandro Del Maschio^{1,2} MD, Francesco De Cobelli^{1,2} MD.

¹ Unit of Clinical Research in Radiology, Experimental Imaging Center, IRCCS Ospedale San Raffaele, Milano, Italy

² Vita-Salute San Raffaele University, Milano, Italy

³ University Centre of Statistics in the Biomedical Sciences, Vita-Salute San Raffaele University, Milan, Italy

⁴ Unit of Radiotherapy, IRCCS Ospedale San Raffaele, Milano, Italy

⁵ Department of Pathology, IRCCS Ospedale San Raffaele, Milano, Italy

⁶ Medical Physics, San Raffaele Hospital, Milano, Italy

⁷ Department of Gastrointestinal Surgery, San Raffaele Hospital, Milano, Italy

Address for correspondence:

Anna Palmisano, M.D.

Experimental Imaging Center, San Raffaele Scientific Institute

Via Olgettina 60, 20132, Milano, Italy

Tel. +39 02 2643 6102; Fax. +39 02 2643 2165

e-mail: palmisano.anna@hsr.it

Author Contributions

1 guarantor of integrity of the entire study: Francesco De Cobelli

2 study concepts and design: Anna Palmisano, Francesco De Cobelli

3 literature research: Anna Palmisano , Alessandra Di Chiara, Antonio Esposito

4 clinical studies: Anna Palmisano, Alessandra Di Chiara, Antonio Esposito, Claudio Fiorino, Paolo Passoni, Luca Albarello, Riccardo Rosati, Alessandro Del Maschio, Francesco De Cobelli.

5 experimental studies / data analysis: Anna Palmisano , Alessandra Di Chiara

6 statistical analysis: Paola Maria Vittoria Rancoita

7 manuscript preparation: Anna Palmisano, Antonio Esposito

8 manuscript editing: Anna Palmisano, Alessandra Di Chiara, Antonio Esposito, Claudio Fiorino, Paolo Passoni, Luca Albarello, Riccardo Rosati, Alessandro Del Maschio, Francesco De Cobelli.

EDITOR'S COMMENTS:

Dear Authors

Please provide pictorial examples of the tumour volume delineation.

Answer: According to Editor' suggestion pictorial examples of the tumour volume delineation in each MRI sequence was added (Figure 1).

REVIEWERS' COMMENTS:

Reviewer #1:

-Add the uniqueness of this study compared to other studies and discuss the same issue.

Answer: The uniqueness of this study consist in the multiple time-point MR assessment of rectal cancer with histogram analysis of tumour volume on ADC maps. Despite functional imaging based on DWI is considered superior to morphological evaluation for the depiction of tumour aggressiveness and prognosticator, the present study show that different imaging parameters are useful in the prediction and monitoring of the degree of response according to the phase of treatment in which MR is performed influence

The aim was rephrased at the end of introduction in order to emphasize these aspects, as well as discussion.

-Add more about basic of routine and advanced DWI modules using this ref
Abdel Razek AAK. Routine and Advanced Diffusion Imaging Modules of the Salivary Glands. Neuroimaging Clin N Am 2018;28:245-254.

Answer: According to reviewer' suggestion more about DWI modules was added using the aforementioned reference. Specifically, about histogram and texture analysis in the introduction (lines 53-56) and in discussion (lines 201-212) and about intravoxel incoherent motion and diffusion kurtosis imaging in discussion (lines 221-226)

-English language correction through the manuscript

Answer: According to reviewer' suggestion the manuscript was edited by a mother tongue speaker.

-Discuss merits and limitations of histogram in discussion

Answer: according to reviewer' suggestion merits and limitation of histogram analysis are added in discussion (lines 201-212 and 221-226).

-Update of references as most of references are old using these ref

Abd-El Khalek Abd-ALRazek A, Fahmy DM. Diagnostic Value of Diffusion-Weighted Imaging and Apparent Diffusion Coefficient in Assessment of the Activity of Crohn Disease: 1.5 or 3 T. *J Comput Assist Tomogr* 2018;42:688-696.

Answer: References were updated and the suggested reference added.

Reviewer #2: Line 33:complete response to CRT, organ-preserving strategies such as 'watch-and-wait' policy may be considered as safe alternatives to major surgery. This is not a safe option and remains controversial, especially in young fit patients. The risk of metastases is 8% and local regrowth is 25% as published in the mentioned paper.

Answer: We agree with the reviewer's comment and we modify the first paragraph of introduction as follows:

"Neoadjuvant chemoradiation therapy (CRT) for the treatment of locally advanced rectal cancer (LARC) leads to a pathological complete response (pCR) in approximately 15–27% of patients [1], suggesting the possibility of tailoring surgical treatment based on individuals' clinical characteristics and the risk of local tumour recurrence or distant metastasis, and eventually applying less-invasive strategy or a 'watch-and-wait' policy in selected cases".

One patient with an entirely mucinous tumour was excluded. The authors did not mention if there was any mucinous component in any of the resected patients. This will have an effect on ADC and sometimes T2 as tumours are difficult to delineate.

Answer: At pretreatment none of the tumour included in the analysis showed mucinous component. The same on MR studies performed during treatment. Only 2 patients showed mucin pools at post-treatment MRI that were confirmed at histological evaluation. Mucin pool at post treatment is a marker of treatment response, indeed both patients were responders (one patients had a complete response, the other had a partial response). Mucinous component were embedded into fibrotic tissue or viable tissue in complete and partial responders, respectively, and the usage of endorectal filling allowed an easier delineation of residual tissue or tumour bed. Mucin components is known to increase ADC values, and higher ADC values could be expected in responders. However, in our sample we did not find higher ADC values after treatment among the three classes of response, probably because of a prevalence in fibrotic evolution which tend to decrease ADC values, balancing the ADC increase related to mucin pools.

The authors should show examples of tumour volume drawings to help the reader understand the concept.

Answer: In accordance to Editor's and reviewer' suggestion pictorial examples of the tumour volume delineation in each MRI sequence was added.

MRI prediction of pathological response in locally advanced rectal cancer: when ADC radiomics meets conventional volumetry

ABSTRACT

Purpose: To investigate the role of DWI-images, T2w-images and ADC histogram analysis before, during and after neoadjuvant chemo-radiotherapy (CRT) in the prediction of pathological response in patients with locally advanced rectal cancer (LARC).

Methods: 1.5T MRI was performed in 43 patients with LARC before, during and after CRT. Tumour volume was measured on both T2-weighted (V_{T2w}) and on DWI b_{1000} images ($V_{b,1000}$) at each time point, hence tumour volume reduction rate (ΔV_{T2w} and $\Delta V_{b,1000}$) was calculated. Whole lesion (3D) first order texture analysis of ADC map was performed. Imaging parameters were compared to pathological Tumour Regression Grade (TRG). The diagnostic performance of each parameter in the identification of complete responders (CR:TRG4), partial responders (PR:TRG3) and no responders (NR:TRG 0-2) was evaluated by multinomial regression analysis and receiver operating characteristics curves.

Results: After surgery 11 patients resulted CR, 22 PR, 10 NR. Before CRT, predictor of CR resulted ADC 75^o percentile and median, with good accuracy (74% and 86%, respectively) and sensitivity (73% and 82%, respectively). During CRT, best predictor of CR resulted ΔV_{T2w} (-58.3%) with good accuracy (81%) and excellent sensitivity (91%). After CRT, best predictors of CR resulted ΔV_{T2w} (-82.8%) and $\Delta V_{b,1000}$ (-86.8%), with 84% of accuracy in both cases and 82% and 91% of sensitivity, respectively.

Conclusions: Median ADC value at pre-treatment MRI and ΔV_{T2w} (from pre-to-during CRT MRI) may have a role in early and accurate prediction of response to treatment. Both ΔV_{T2w} and $\Delta V_{b,1000}$ (from pre-

to-post CRT) help in the identification of CR after CRT.

1 **MRI prediction of pathological response in locally advanced rectal cancer: when ADC radiomics**
2 **meets conventional volumetry**

3 **Keywords:**

- 4 • Rectal cancer
- 5 • Functional Magnetic Resonance Imaging
- 6 • Treatment
- 7 • Neoadjuvant therapy
- 8 • Prognosis

9

10 **Abbreviations and acronyms:**

- 11 ADC: Apparent Diffusion Coefficient
- 12 AUC: Area Under the Curve
- 13 CR: Complete Responders
- 14 CRT: ChemoRadiation Therapy
- 15 DWI: Diffusion Weighted Imaging
- 16 Early ΔV : early Tumour Volume Reduction Rate (from pre-to-during CRT)
- 17 LARC: Local Advanced Rectal Cancer
- 18 Late ΔV : late Tumour Volume Reduction Rate (from pre-to-post CRT)
- 19 NR: No Responders
- 20 pCR: pathological Complete Response

21 PR: Partial Responders

22 ROC: Receiver Operating Characteristics curve

23 ROI: Region Of Interest

24 TRG: Tumour Regression Grade

25

26

27 **INTRODUCTION**

28 Neoadjuvant chemoradiation therapy (CRT) for the treatment of locally advanced rectal cancer
29 (LARC) leads to a pathological complete response (pCR) in approximately 15–27% of patients [1],
30 suggesting the possibility of tailoring surgical treatment based on individuals' clinical characteristics
31 and the risk of local tumour recurrence or distant metastasis, and eventually applying less-invasive
32 strategy or a 'watch-and-wait' policy in selected cases [2, 3]

33 Therefore, a higher accuracy in the prediction of treatment response and in the identification of residual
34 cancer after CRT is required.

35 Magnetic Resonance Imaging (MRI) is widely adopted for rectal cancer staging for its high accuracy in
36 depicting local invasion providing useful information to guide treatment strategy.

37 Unfortunately, MRI performances is suboptimal for restaging and predicting of pathological response.
38 Tumour volume reduction rate evaluated on T2-weighted MRI showed variable results in the
39 assessment of treatment response [4-6], mainly due to the limitation of T2-weighted images in
40 distinguishing radiation-induced fibrosis and peritumoral inflammation from residual cancer [7].

41 On contrary, Diffusion Weighted Imaging (DWI) significantly improves rectal cancer restaging, by
42 providing information about tissue microarchitecture mostly related to cellular density [8,9], which is
43 higher in malignancies and more aggressive cancers [9-11].

44 Apparent Diffusion Coefficient (ADC) is a biomarker of malignancy. In rectal cancer ADC is
45 associated with cell count, Ki67 [12] and histological features [13], but its role in prediction and
46 monitoring of LARC response to CRT is still controversial [4, 14-17]. The main reason for such
47 discrepancy lies in methodological differences such as non-standardized DWI sequences and image
48 post-processing [4,9,14-18], which impacts on data reproducibility [19, 20].

49 Moreover, rectal cancer has been characterized by a certain degree of inherent heterogeneity, which is
50 related to tumour aggressiveness and prognosis; thus the simple evaluation of mean ADC values has
51 the potential bias of overlooking tumour heterogeneity. A strategy to overcome this limitation consist
52 in the extraction of parameters describing inherent ADC heterogeneity through histogram analysis [21-
53 23]. Histogram analysis consists of first order statistics describing the frequency distribution of
54 intensity values within a ROI or VOI [23] revealing subtle microstructural alterations, that are invisible
55 to the naked eye. ADC histogram parameters resulted related to histological features [13] and
56 potentially to the degree of response to treatment [18].

57 In a recent study, it was demonstrated that MR monitoring of rectal cancer during CRT may effectively
58 detect responders in the early phase of treatment [24], however, only T2 volumetry was assessed.

59 Based on the knowledge that DWI may improve MRI diagnostic performances after CRT [9, 11] and
60 that histogram analysis may identify ADC diffusivity pattern related to sensitivity to CRT [18], the
61 present study aimed to identify the best imaging predictor of treatment response before, during and
62 after CRT using multiparametric MRI evaluation including volumetric assessment on T2 and DWI and
63 volumetric ADC histogram analysis.

64

65 MATERIAL AND METHODS

66 Patient demographics

67 The Institutional Review Board approved this prospective observational study and written informed
68 consent was obtained. Between January 2013 and March 2018, 56 consecutive patients with
69 histologically proven LARC who received neoadjuvant CRT, underwent MRI prior to CRT (pre-MRI),
70 during CRT (mid-MRI) and 8 weeks after CRT (post-MRI). Thirteen out of 56 patients were excluded
71 because of (a) MRI artefacts (n = 2), (b) tumour with an entirely mucinous aspect (n = 1), (c) the lack
72 of DWI at each time point (n = 5), (d) different CRT scheme (n = 5). The study population is
73 summarized in Table 1.

74 MRI protocol

75 MRI examinations were performed on a 1.5-T magnet (Ingenia, Philips Medical Systems, Best The
76 Netherlands) equipped with a 32-channel phased array body coil. Patients were prepared with
77 endorectal filling (50 cc of Lumirem®, Guerbet S.p.A.) and intramuscular injection of
78 butylscopolamine (20 mg) to reduce bowel peristalsis.

79 The imaging protocol included:

- 80 - High-resolution TSE T2-weighted sequences (TR 5531 msec; FOV 240x240x76 mm; matrix
81 512x512; slice thickness 3 mm; gap 0.3 mm; turbo factor 12) oriented on the three orthogonal
82 planes.

- 83 - DWI single-shot echo-planar sequence in the axial plane (TR 3768 ms; TE 72 ms; FOV
84 260x260x119 mm; 30 slices; slice thickness 3 mm; gap: 1 mm; NSA 8) with four different b
85 values (0, 200, 600, 1000).
- 86 - 3D T1-weighted TFE sequences with fat suppression (TR 4.4 ms; TE = 4.1 ms; matrix = 336 ×
87 336; NSA = 1; 20 dynamics) acquired during intravenous injection of 0.1 mL/kg of body
88 weight of gadobutrol.

89 **Image analysis**

90 Two readers [REDACTED] with 5 and 8 years of experience in oncologic body imaging, blinded to
91 the histopathology results, independently drew the whole-tumour volume at pre, mid and post-MRI by
92 manually tracing the outer edge of the lesion on high-resolution axial-T2-weighted and $DWI_{b,1000}$
93 images using a dedicated software (Olea Medical Software, La Ciotat, France) (Figure 1). The
94 extracted parameters were: total volume segmented on T2w (V_{T2w}) and $DWI_{b,1000}$ ($V_{b,1000}$) images, early
95 tumour volume reduction rate (early ΔV) on both T2w and $DWI_{b,1000}$ images ($(V_{pre-MRI} - V_{mid-}$
96 $MRI) / V_{pre-MRI} \times 100$) and late tumour volume reduction rate (late ΔV) on both T2w and $DWI_{b,1000}$
97 images ($(V_{pre-MRI} - V_{post-MRI}) / V_{pre-MRI} \times 100$).

98 V_{T2w} was automatically co-registered to ADC map, and manually corrected. If no residual tumour was
99 identified after therapy, the volume was drawn in the apparent tumour bed. The following parameters
100 describing the histogram of ADC values in the entire tumour (3D-ADC) were recorded: 25th, 50th,
101 75th percentile, mean, skewness and kurtosis. The two readers independently traced a single region of
102 interest (ROI) along tumour edges on a representative section and a small round-shaped ROI on a
103 darker area of the tumour in order to obtain the single-section (ss-ADC) and restricted ADC (r-ADC)
104 values, respectively.

105 **Chemoradiation therapy**

106 Oxaliplatin 100mg/m² and 5-Fluorouracil (5-FU) 200 mg/m²/day were administered from 14 days
107 before RT to the end of RT cycle. Radiation therapy consisted of tomotherapy (total dose 41.4 Gy in 18
108 fractions: 2.3 Gy per fraction) delivered to a planning target volume including the tumour and regional
109 lymph nodes defined on pre-MRI. In the last 6 fractions an additional boost of 3.1 Gy per fraction was
110 delivered to the residual cancer recognized on mid-MRI [25].

111 **Pathologic assessment of response**

112 Surgically resected specimens were examined by L.A. (15 years of experience), according to the 7th
113 American Joint Committee on Cancer TNM staging system and tumour regression grade (TRG) Rödel
114 classification [26]. Pathological complete response was defined as the absence of viable tumour cells in
115 the primary tumour and lymph nodes. Patients were classified as follow: TRG0-2 as no responders
116 (NR), TRG3 as partial responders (PR), TRG4 as complete responders (CR).

117 **Statistical analysis**

118 Correlations among features were calculated using the Spearman correlation coefficient.

119 Kruskal-Wallis' test followed by a post-hoc analysis with Dunn's test was utilized to compare the
120 means of the parameters in the three classes of pathological response (NR, PR and CR). The
121 performance of the parameters in predicting the three types of response was evaluated by using
122 univariate multinomial regression. In both the analysis, p-values were adjusted for multiple
123 comparisons using Bonferroni's correction.

124 The Receiver Operating Characteristics (ROC) curve analysis was used to investigate the performance
125 of the parameters in predicting either CR or NR. The Area Under the Curve (AUC) was analysed to
126 compare the performances. AUC above 0.8 was considered good, while values between 0.7 and 0.8

127 was considered acceptable. The optimal cut-off of each variable was derived using the standard
128 method, and was considered as the point closest to the upper left corner of the ROC curve.
129 P-value less than 0.05 was considered statistically significant. All statistical analyses were performed
130 using R software, version 3.2.0 (<http://www.R-project.org/>).

131 **RESULTS**

132 **Patient characteristics**

133 According to the pathological TRG, out of 43 patients, 11 (26%) were recognized as CR, 22 (51%) as
134 PR and 10 (23%) as NR.

135 Radiological stages on pre-MRI and histopathological findings are summarized in Table 1.
136

137 **Tumour volumetry on T2w and high b-value images: differences among groups**

138 Figure 2 showed V_{T2w} and $V_{b,1000}$ at pre-MRI (A, B), mid-MRI (C, D) and post-MRI (E, F) according
139 to the pathological TRG.

140 At pre-MRI, both V_{T2w} and $V_{b,1000}$ resulted no significantly different among classes of response,
141 regardless a tendency to smaller volumes in CR.

142 CR had lower V_{T2w} in comparison to NR at mid-MRI, (Fig.2, Table 2) and lower V_{T2w} and $V_{b,1000}$ with
143 respect to PR and NR at post-MRI (Fig.2, Table 2).

144 There was no significant difference in tumour volume (V_{T2w} and $V_{b,1000}$) between PR and NR at each
145 time-point.

146 Tumour volume values obtained from T2w images segmentation at pre-MRI strongly agree with
147 tumour volume segmentation on $DWI_{b,1000}$ ($p:0.8960$, $p<0.0001$); while an acceptable agreement was

148 observed at mid-MRI and post-MRI ($p=0.7558$, $p<0.0001$ and $p=0.7228$, $p<0.0001$, respectively).

149 Both early (pre-to-during CRT) and late (pre-to-post CRT) tumour volume reduction rate ΔV_{T2w} (Table
150 2, Figure 3) were significantly different among different classes of responses ($p=0.0006$ and $p=0.0019$,
151 respectively).

152 In particular CR presented a higher median early ΔV_{T2w} compared to PR (CR:-75% vs PR:-49%,
153 $p=0.0019$) and NR (CR:-75% vs NR:-38%, $p=0.0001$), as well as higher late ΔV_{T2w} in comparison to
154 PR (CR:-86% vs PR:-75%, $p=0.0034$) and NR (CR:-86% vs NR:- 59%, $p=0.0003$).

155 The median early $\Delta V_{b,1000}$ was not statistically different among classes of response (CR: -77% vs PR:-
156 58% vs NR: -41%, $p=0.4979$). Late $\Delta V_{b,1000}$ was significantly higher in CR with respect to PR (CR:-
157 97% vs PR:-78%; $p=0.0023$) and NR (CR:-97% vs NR: -69%; $p=0.0001$).

158 Among all volumetric parameters, only the following variables were obtained as significant predictors
159 of the pathological response (CR, PR, NR): early and late ΔV_{T2w} ($p=0.0028$ and $p=0.0090$,
160 respectively), late $\Delta V_{b,1000}$ ($p=0.0265$) (Table 3).

161 Table 4 and Figure 4 show the best cut-off of these predictors to discriminate between CR and NR
162 groups-

163 All three parameters showed good performances in the prediction of CR (AUC always >0.80), and
164 acceptable (AUC 0.70-0.80) in the prediction of NR.

165 In particular, to predict the CR, early ΔV_{T2w} showed a comparable accuracy to late ΔV_{T2w} and late
166 $\Delta V_{b,1000}$, with a sensitivity equal to $\Delta V_{b,1000}$ and higher than ΔV_{T2w} (Table 4).

167 **3D-ADC histogram-based analysis**

168 Only at pre-MRI, 3D-ADC mean values were significantly different among the three groups of

169 response to treatment (median [IQR]: $1.07 [1.03;1.17] \times 10^{-3} \text{ mm}^2/\text{s}$ in NR, $1.14 [1.06;1.2] \times 10^{-3} \text{ mm}^2/\text{s}$
170 in PR and $1.27 [1.22;1.34] \times 10^{-3} \text{ mm}^2/\text{s}$ in CR, $p=0.0079$), which was higher in CR than PR and NR
171 ($p=0.0042$ and $p=0.0029$, respectively), but not significantly different between PR and NR ($p=0.7696$)
172 (Fig. 5A). At mid-MRI and post-MRI, 3D-ADC mean value significantly increased with respect to pre-
173 MRI in the NR and PR patients (Figure 5D and E).

174 At multinomial regression analysis, only 75^opercentile and 3D-ADC median at pre-MRI, were positive
175 predictors of response to treatment ($p=0.0247$ and $p=0.0415$, respectively) (Table 3).

176 Moreover, none of the parameters obtained at mid-MRI and post-MRI was presented as the predictor of
177 response to treatment.

178 ROC curves and the best cut-offs for prediction of pathological response are reported in Fig.4C and D,
179 and Table 4.

180 **Interobserver agreement**

181 The two readers strongly agreed when measuring V_{T2w} , $V_{b,1000}$ and 3D-ADC values of rectal tumour.
182 Inter-observer agreement for V_{T2w} tend to reduce overtime, varying from excellent at pre-MRI (ρ :
183 0.9236 , $p<0.0001$) to good at mid-MRI (ρ : 0.8203 , $p<0.0001$), and moderate at post-MRI (ρ : 0.7214 ,
184 $p<0.0001$).

185 Inter-observer agreement was excellent for $V_{b,1000}$ measurement at pre-MRI (ρ : 0.9338 , $p<0.0001$) and
186 mid-MRI (ρ : 0.8983 , $p<0.0001$), good at post-MRI (ρ : 0.8357 , $p<0.0001$). Furthermore it was excellent
187 for 3D-ADC analysis at each time-point (pre-MRI ρ : 0.9124 , $p<0.0001$; mid-MRI ρ : 0.9047 ,
188 $p<0.0001$;post-MRI ρ : 0.9056 , $p<0.0046$) .

189 **DISCUSSION**

190 In the present study, we found that: (i) 3D-ADC histogram analysis at pre-MRI seems to be able to
191 identify those lesions with higher possibility of gaining a complete response to neoadjuvant CRT; (ii)
192 early ΔV_{T2w} is effective in the early prediction of response during CRT; (iii) High b-value (b1000)
193 volumetry may improve the accuracy in identifying the residual tumour at post-MRI.

194 ADC is an established imaging biomarker of tumour aggressiveness and prognosis, and lower values
195 were associated with more aggressive phenotype [27, 28]. Similarly, in our setting, a lower ADC mean
196 value before CRT was reported in patients with poor response to treatment. Nevertheless, ADC mean
197 was not obtained as predictor of response to treatment, differently from 75th percentile and 3D-ADC
198 median values ($p = 0.0247$ and $p = 0.0415$, respectively). In particular, 3D-ADC median showed
199 diagnostic performances higher than 80%. Considering the fact that the median value represents as a
200 middle value in set of volume ranges, it probably better depicts cancer behaviour rather than mean
201 value, resulting consequently the more robust ADC parameter predicting treatment response with good
202 performances and potentially useful to guide a tailored treatment.

203 In fact, considering the high inherent heterogeneity of rectal cancer, the usage of summary statistics,
204 such as mean ADC value, is affected by the risk to overlook tumour heterogeneity, which is a factor
205 impacting on treatment response [13, 18, 22, 29].

206 However, histogram analysis describes the frequency distribution of intensity within the ROI, without
207 accounting for local relationship between pixels, which can be measured using higher order texture
208 analysis [23, 30].

209 Despite the potential advantage of higher order statistics to better reflect intratumoral heterogeneity for
210 accounting for spatial relationship of pixels and its promising results in the identification of subtle
211 microstructural alteration [31, 32], in the setting of rectal cancer more stability and higher
212 reproducibility of data was found from I order texture analysis (histogram analysis) of ADC map [30].

213 being less sensitive to manual tumour delineation differences, image noise, pixel size resampling and
214 intensity discretization [30].

215 The robustness of results is supported by excellent inter-observer agreement for 3D-ADC at each time-
216 point suggesting the high reproducibility of the volumetric approach, which is in accordance with
217 recent findings [19, 20, 33, 34]

218 ADC values increased during and after treatment as consequence of cellular damage with disruption of
219 cell membranes, however, without significant differences among the classes of response.

220 In some report a significant improvement of ADC values was reported in complete responders, but this
221 finding was not always confirmed [4, 35-37], as in our study. This could be explained by the co-
222 presence of multiple phenomena such as inflammation, fibrosis, acute cellular swelling, and fat
223 infiltration that may significantly hide ADC values changes strictly related to reduction of neoplastic
224 cells. Probably, the application of advanced diffusion techniques to fit the non-Gaussian diffusion
225 curve of water molecule including intravoxel incoherent motion and diffusion kurtosis imaging [23]
226 may improve the evaluation of treatment response for a potentially better depiction of neoplastic cells
227 integrity in the complex tumour environment. Despite the encouraging results [38-40], these
228 approaches are not widely performed and need long acquisition time and further investigation for
229 generalizability of results [41].

230 Only early ΔV_{T2w} was able to distinguish the rectal cancer response to treatment during CRT. Early
231 ΔV_{T2w} predicted CR with a comparable accuracy in comparison to late ΔV_{T2w} (from pre-to-post CRT)
232 (81% vs 84%) but with higher sensitivity (91% vs 82%), associated with the advantage of an earlier
233 assessment. This result confirm recent findings [24], and suggest the possibility of effectively
234 identifying the degree of response in the earliest phases of treatment by performing a fast MRI protocol
235 including only T2weighted images, without the necessity of additional sequences and/or contrast
236 media.

237 The reason of the higher sensitivity of early ΔV_{T2w} probably lies in the easier distinguishing of viable
238 tumour at mid-MRI with respect to post-MRI [42] due to the less evident desmoplastic reaction.
239 At post-MRI, both ΔV_{T2w} and $\Delta V_{b,1000}$ had a role in the identification of CR, but $\Delta V_{b,1000}$ showed
240 higher sensitivity (91%) and a major reduction rate ($\Delta V_{b,1000} > -97\%$), due to a clear-cut delineation of
241 tumor on $DWI_{b,1000}$, supporting the utility of DWI in restaging MRI [4, 43, 44].
242 The absence of a complete disappearance of signal on high b values images at post-MRI which were
243 misdiagnosed as residual tumour volume, is explained by T2 shine-through effects for persistence of
244 intraluminal fluid and collapsed rectal wall [45].
245 As expected, late ΔV_{T2w} showed lower sensitivity respect to $\Delta V_{b,1000}$ in the identification of complete
246 responders, for challenge discrimination of viable tumour from fibrosis and inflammation [7,42].
247 However, the late ΔV_{T2w} cut-off value for prediction of response and also its accuracy are in line with
248 the data previously published in a meta-analysis by Martens et al. [46].
249 Our study has some limitations. A relatively small cohort of patients was enrolled. However, to avoid
250 the risk of overfitting the data, multiplicity adjustment was applied and only robust data was taken into
251 consideration. The lack of biomarkers of tumour cell proliferation, hypoxia, and angiogenesis is
252 another limitation since the histopathological evaluation was performed only after surgery.

253 In conclusion, our study suggests that different parameters have a different role in prediction of
254 response related to the exact MRI acquisition time with respect to treatment phases. DWI is useful for
255 the characterization of tumour behaviour before treatment, as well as in the identification of residual
256 cancer after CRT, where simple volumetric evaluation is enough and highly accurate. Histogram
257 analysis resulted more robust than ADC mean values assessment, with median ADC values as predictor
258 of response at pretreatment MRI. Finally, tumour volume modification on T2w images from pre-to-
259 during treatment resulted the unique predictor of response during treatment, resulting able to early and
260 accurately identify different degree of response, and potentially useful to tailor patient's treatment.

261 REFERENCES:

- 262 1. Maas M, Nelemans PJ, Valentini V et al. Long-term outcome in patients with a pathological
263 complete response after chemoradiation for rectal cancer: a pooled analysis of individual patient data.
264 *Lancet Oncol* 2010; 11: 835-844.
- 265 2. van der Valk MJ, Hilling DE, Bastiaannet E et al. Long-term outcomes of clinical complete
266 responders after neoadjuvant treatment for rectal cancer in the International Watch & Wait Database
267 (IWWD): an international multicentre registry study. *Lancet* 2018; 391: 2537-2545.
- 268 3. Maas M, Beets-Tan RGH, Lambregts DMJ et al. Wait-and-See Policy for Clinical Complete
269 Responders After Chemoradiation for Rectal Cancer. *J Clin Oncol* 2011; 29: 4633-4640.
- 270 4. Curvo-Semedo L, Lambregts DM, Maas M et al. Rectal cancer: assessment of complete
271 response to preoperative combined radiation therapy with chemotherapy—conventional MR volumetry
272 versus diffusion-weighted MR imaging. *Radiology* 2011; 260: 734-743.
- 273 5. Patel UB, Brown G, Rutten H et al. Comparison of magnetic resonance imaging and
274 histopathological response to chemoradiotherapy in locally advanced rectal cancer. *Ann Surg Oncol*
275 2012; 19: 2842-2852.
- 276 6. Xiao J, Tan Y, Li W et al. Tumor volume reduction rate is superior to RECIST for predicting
277 the pathological response of rectal cancer treated with neoadjuvant chemoradiation: Results from a
278 prospective study. *Oncol Lett* 2015; 9: 2680-2686.
- 279 7. Patel UB, Blomqvist LK, Taylor F et al. MRI after treatment of locally advanced rectal cancer:
280 how to report tumor response—the MERCURY experience. *AJR* 2012; 199: W486-W495.
- 281 8. Abd-El Khalek Abd-Alrazek A, Fahmy DM. Diagnostic Value of Diffusion-Weighted Imaging
282 and Apparent Diffusion Coefficient in Assessment of the Activity of Crohn Disease: 1.5 or 3 T. *Journal*
283 *of computer assisted tomography* 2018; 42: 688-696.
- 284 9. Schurink NW, Lambregts DMJ, Beets-Tan RGH.. Diffusion-weighted Imaging in Rectal
285 Cancer: Current Applications and Future Perspectives. *Br J Radiol* 2019; 92 (1096): 20180655.
- 286 10. Sun Y, Tong T, Cai S et al. Apparent diffusion coefficient (ADC) value: a potential imaging
287 biomarker that reflects the biological features of rectal cancer. *PLoS One* 2014; 9: e109371.
- 288 11. Beets-Tan RG, Lambregts DM, Maas M et al. Magnetic resonance imaging for clinical
289 management of rectal cancer: updated recommendations from the 2016 European Society of
290 Gastrointestinal and Abdominal Radiology (ESGAR) consensus meeting. *Eur Radiol* 2018; 28: 1465-
291 1475.
- 292 12. Surov A, Meyer HJ, Wienke A. Associations between apparent diffusion coefficient (ADC) and
293 KI 67 in different tumors: a meta-analysis. Part 1: ADC(mean). *Oncotarget* 2017; 8: 75434-75444.
- 294 13. Meyer HJ, Hohn A, Surov A. Histogram analysis of ADC in rectal cancer: associations with
295 different histopathological findings including expression of EGFR, Hif1-alpha, VEGF, p53, PD1, and
296 KI 67. A preliminary study. *Oncotarget* 2018; 9: 18510-18517.
- 297 14. Napoletano M, Mazzucca D, Prosperi E et al. Locally Advanced Rectal Cancer: Qualitative and
298 Quantitative Evaluation of Diffusion-Weighted Magnetic Resonance Imaging in Restaging After
299 Neoadjuvant Chemo-Radiotherapy. *Abdom Radiol.* 2019 Nov;44(11):3664-3673.
- 300 15. Tarallo N, Angeretti MG, Bracchi E et al. D Magnetic Resonance Imaging in Locally Advanced
301 Rectal Cancer: Quantitative Evaluation of the Complete Response to Neoadjuvant Therapy. *Pol J*
302 *Radiol.* 2018 Dec 17;83:e600-e609. .
- 303 16. Xie H, Sun T, Chen M et al. Effectiveness of the apparent diffusion coefficient for predicting
304 the response to chemoradiation therapy in locally advanced rectal cancer: a systematic review and
305 meta-analysis. *Medicine (Baltimore)* 2015 Feb;94(6):e517.

- 306 17. Lambrecht M, Vandecaveye V, De Keyzer F et al. Value of diffusion-weighted magnetic
307 resonance imaging for prediction and early assessment of response to neoadjuvant radiochemotherapy
308 in rectal cancer: preliminary results. *International journal of radiation oncology, biology, physics* 2012;
309 82: 863-870.
- 310 18. Enkhbaatar NE, Inoue S, Yamamuro H et al. MR Imaging with Apparent Diffusion Coefficient
311 Histogram Analysis: Evaluation of Locally Advanced Rectal Cancer after Chemotherapy and Radiation
312 Therapy. *Radiology* 2018; 288: 129-137.
- 313 19. Blazic IM, Lilic GB, Gajic MMJR. Quantitative assessment of rectal cancer response to
314 neoadjuvant combined chemotherapy and radiation therapy: comparison of three methods of
315 positioning region of interest for ADC measurements at diffusion-weighted MR imaging. *Radiology*
316 2016; 282: 418-428.
- 317 20. Yang P, Xu C, Hu X et al. Reduced Field-of-View Diffusion-Weighted Imaging in Histological
318 Characterization of Rectal Cancer: Impact of Different Region-of-Interest Positioning Protocols on
319 Apparent Diffusion Coefficient Measurements. *Eur J Radiol* 2020; 127: 109028.
- 320 21. Yang L, Qiu M, Xia C et al. Value of High-Resolution DWI in Combination With Texture
321 Analysis for the Evaluation of Tumor Response After Preoperative Chemoradiotherapy for Locally
322 Advanced Rectal Cancer. *AJR Am J Roentgenol* 2019; 1-8.
- 323 22. Palmisano A, Esposito A, Rancoita PMV et al. Could perfusion heterogeneity at dynamic
324 contrast-enhanced MRI be used to predict rectal cancer sensitivity to chemoradiotherapy? *Clin Radiol*
325 2018; 73: 911.e911-911.e917.
- 326 23. Abdel Razek AAK. Routine and Advanced Diffusion Imaging Modules of the Salivary Glands.
327 *Neuroimaging Clin N Am* 2018; 28: 245-254.
- 328 24. Palmisano A, Esposito A, Di Chiara A et al. Could early tumour volume changes assessed on
329 morphological MRI predict the response to chemoradiation therapy in locally-advanced rectal cancer?
330 *Clin Radiol* 2018; 73: 555-563.
- 331 25. Passoni P, Fiorino C, Slim N et al. Feasibility of an adaptive strategy in preoperative
332 radiochemotherapy for rectal cancer with image-guided tomotherapy: boosting the dose to the
333 shrinking tumor. *Int J Radiat Oncol Biol Phys.* 2013; 87: 67-72.
- 334 26. Rodel C, Martus P, Papadopoulos T et al. Prognostic significance of tumor regression after
335 preoperative chemoradiotherapy for rectal cancer. *J Clin Oncol.* 2005; 23: 8688-8696.
- 336 27. Moon SJ, Cho SH, Kim GC et al. Complementary value of pre-treatment apparent diffusion
337 coefficient in rectal cancer for predicting tumor recurrence. *Abdom Radiol (NY)* 2016; 41: 1237-1244.
- 338 28. Noda Y, Goshima S, Kajita K et al. Prognostic Value of Diffusion MR Imaging and Clinical-
339 Pathologic Factors in Patients with Rectal Cancer. *Iran J Radiol.* 2018 ; 15(1):e57080.
- 340 29. Just N. Improving tumour heterogeneity MRI assessment with histograms. *Br J Cancer.* 2014;
341 111: 2205.
- 342 30. Traverso A, Kazmierski M, Shi Z et al. Stability of radiomic features of apparent diffusion
343 coefficient (ADC) maps for locally advanced rectal cancer in response to image pre-processing. *Phys*
344 *Med* 2019; 61: 44-51.
- 345 31. Becker AS, Ghafoor S, Marcon M et al. MRI texture features may predict differentiation and
346 nodal stage of cervical cancer: a pilot study. *Acta Radiol Open* 2017; 6: 2058460117729574.
- 347 32. Lu Z, Wang L, Xia K et al. Prediction of Clinical Pathologic Prognostic Factors for Rectal
348 Adenocarcinoma: Volumetric Texture Analysis Based on Apparent Diffusion Coefficient Maps. *J Med*
349 *Syst.* 2019 Nov 7;43(12):331.
- 350 33. Lambregts DM, Beets GL, Maas M et al. Tumour ADC measurements in rectal cancer: effect of
351 ROI methods on ADC values and interobserver variability. *Eur Radiol* 2011; 21: 2567-2574.
- 352 34. Nougaret S, Vargas HA, Lakhman Y et al. Intravoxel incoherent motion-derived histogram
353 metrics for assessment of response after combined chemotherapy and radiation therapy in rectal cancer:

354 initial experience and comparison between single-section and volumetric analyses. *Radiology* 2016;
355 280: 446-454.

356 35. De Felice F, Magnante AL, Musio D et al. Diffusion-weighted magnetic resonance imaging in
357 locally advanced rectal cancer treated with neoadjuvant chemoradiotherapy. *Eur J Surg Oncol* 2017;
358 43: 1324-1329.

359 36. Intven M, Monninkhof EM, Reerink O, Philippens MEP. Combined T2w volumetry, DW-MRI
360 and DCE-MRI for response assessment after neo-adjuvant chemoradiation in locally advanced rectal
361 cancer. *Acta Oncol* . 2015 Nov;54(10):1729-36.

362 37. Foti PV, Privitera G, Piana S et al. Locally advanced rectal cancer: Qualitative and quantitative
363 evaluation of diffusion-weighted MR imaging in the response assessment after neoadjuvant chemo-
364 radiotherapy. *Eur J Radiol Open*. 2016; 3: 145-152.

365 38. Zhang XY, Wang L, Zhu HT et al. Predicting Rectal Cancer Response to Neoadjuvant
366 Chemoradiotherapy Using Deep Learning of Diffusion Kurtosis MRI. *Radiology* 2020; 190936.

367 39. Hu F, Tang W, Sun Y et al. The value of diffusion kurtosis imaging in assessing pathological
368 complete response to neoadjuvant chemoradiation therapy in rectal cancer: a comparison with
369 conventional diffusion-weighted imaging. *Oncotarget* 2017; 8: 75597-75606.

370 40. Cui Y, Cui X, Yang X et al. Diffusion kurtosis imaging-derived histogram metrics for
371 prediction of KRAS mutation in rectal adenocarcinoma: Preliminary findings. *J Magn Reson Imaging*
372 2019; 50: 930-939.

373 41. Koh DM. Using Deep Learning for MRI to Identify Responders to Chemoradiotherapy in
374 Rectal Cancer. *Radiology* 2020; 200417.

375 42. Hanly AM, Ryan EM, Rogers AC et al. Multicenter evaluation of rectal cancer reimaging post
376 neoadjuvant (MERRION) therapy. *Ann Surg*. 2014;259(4):723-7.

377 43. Ha HI, Kim AY, Yu CS et al. Locally advanced rectal cancer: diffusion-weighted MR tumour
378 volumetry and the apparent diffusion coefficient for evaluating complete remission after preoperative
379 chemoradiation therapy. *Eur Radiol*. 2013; 23: 3345-3353.

380 44. Lambregts DM, Rao S-X, Sassen S et al. MRI and Diffusion-weighted MRI volumetry for
381 identification of complete tumor responders after preoperative chemoradiotherapy in patients with
382 rectal cancer. *Ann Surg*. 2015; 262: 1034-1039.

383 45. Lambregts DM, van Heeswijk MM, Pizzi AD et al. Diffusion-weighted MRI to assess response
384 to chemoradiotherapy in rectal cancer: main interpretation pitfalls and their use for teaching. *Eur*
385 *Radiol*. 2017; 27: 4445-4454.

386 46. Martens MH, van Heeswijk MM, van den Broek JJ et al. Prospective, multicenter validation
387 study of magnetic resonance volumetry for response assessment after preoperative chemoradiation in
388 rectal cancer: can the results in the literature be reproduced? *Int J Radiat Oncol Biol Phys*. 2015; 93:
389 1005-1014.

390

391 **TABLE:**

392 **Table 1. Population features**

393 **Table 2. Tumour volumes on T2w images (V_{T2w}) and DWI ($V_{b,1000}$) at each time point, with**

394 **corresponding ΔV during (early ΔV) and post CRT (late ΔV) in relation to pathological response.**

395 Tumour volumes results not significantly different among classes of pathological response at pre-MRI.
396 They differed in term of V_{T2w} at mid-MRI, and in both V_{T2w} and $V_{b,1000}$ at post-MRI. Tumour volume
397 reduction rate (ΔV) was different with respect to response so just during treatment if measured on T2w
398 images, and after treatment at both the evaluation.

399 **Table 3. Univariate multinomial regression for the prediction of the three classes of responders**

400 **Table 4. ROC analysis for prediction of either NR or CR by volumetric and 3D-ADC parameters**
401 **significant at multinomial analysis.**

402

403 **FIGURE LEGEND:**

404 **Figure 1. Volume segmentation and histogram extraction.** Using a dedicated software tumour
405 volume was manually segmented on high resolution T2w images (on top). Hence, using a rigid
406 coregistration, tumour contour and volume obtained on T2w images were copied on b1000 DWI
407 images (image on right) and ADC map (on left on bottom) and manually adjusted. From volumes
408 pixel-by-pixel intensity values were extracted and ADC histogram analysed (on right on bottom).

409 **Figure 2: V_{T2w} and $V_{b,1000}$ according to pathological TRG at pre-MRI (A, B), mid-MRI (C, D),**
410 **and post-MRI(E, F).**

411 Tumour volumes results not significantly different among classes of pathological response at pre-MRI.
412 They differed in term of V_{T2w} at mid-MRI, and in both V_{T2w} and $V_{b,1000}$ at post-MRI. Tumour
413 P-values of Kruskal-Wallis's test were adjusted with Bonferroni's correction.

414 **Figure 3: Tumour volume modification rate during (A, B) and after CRT (C, D). Tumour**

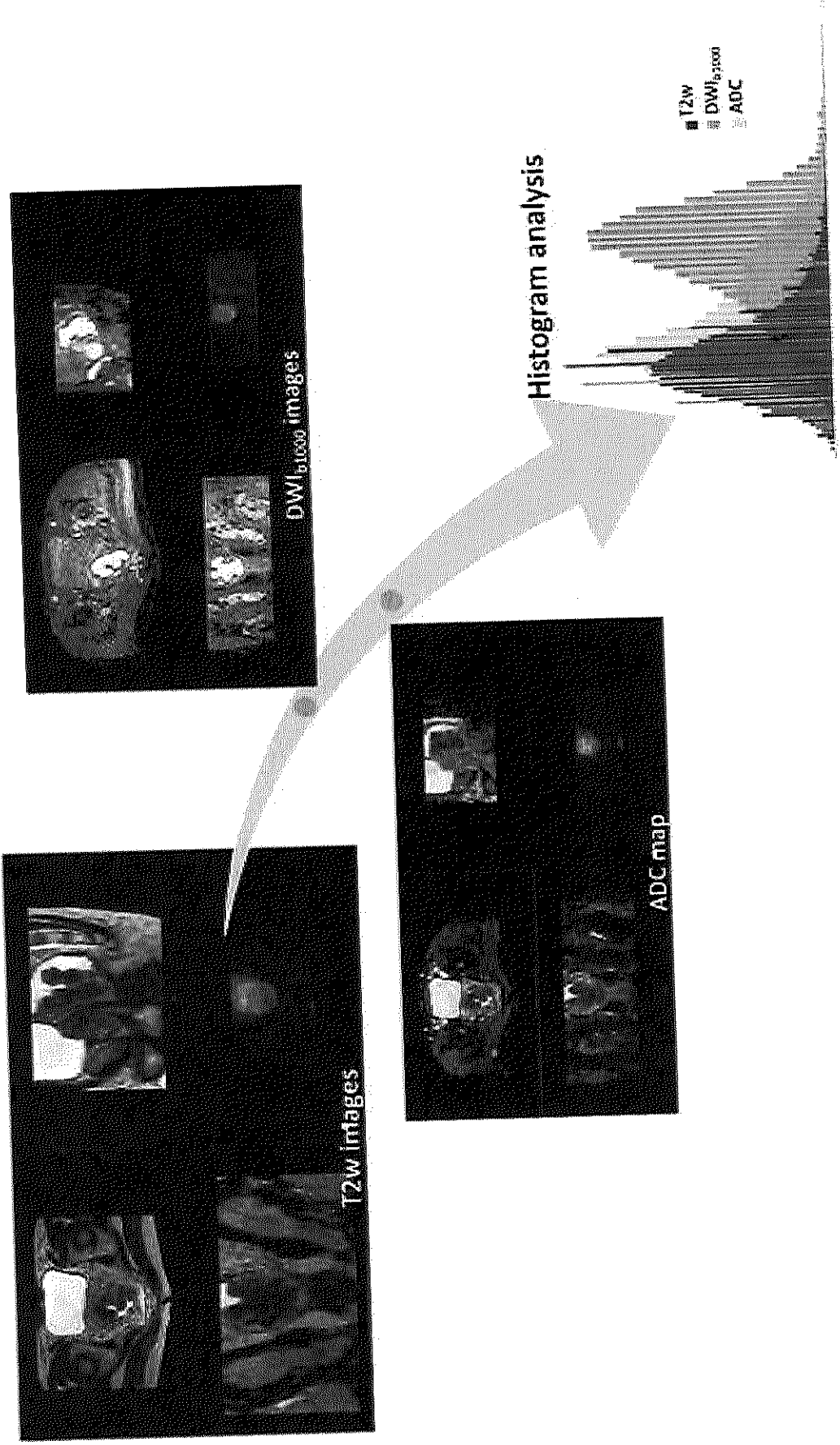
415 reduction rate based on T2w volumetry was significantly different between CR and NR and NR earlier,
416 during CRT. Tumour volume reduction rate was significantly different among classes of response in
417 both T2w and DWI_{b,1000} images.

418 **Figure 4: ROC curves of volumetric parameters (A, B) and ADC texture parameter (C, D)**
419 **significant predictors at multinomial regression analysis.**

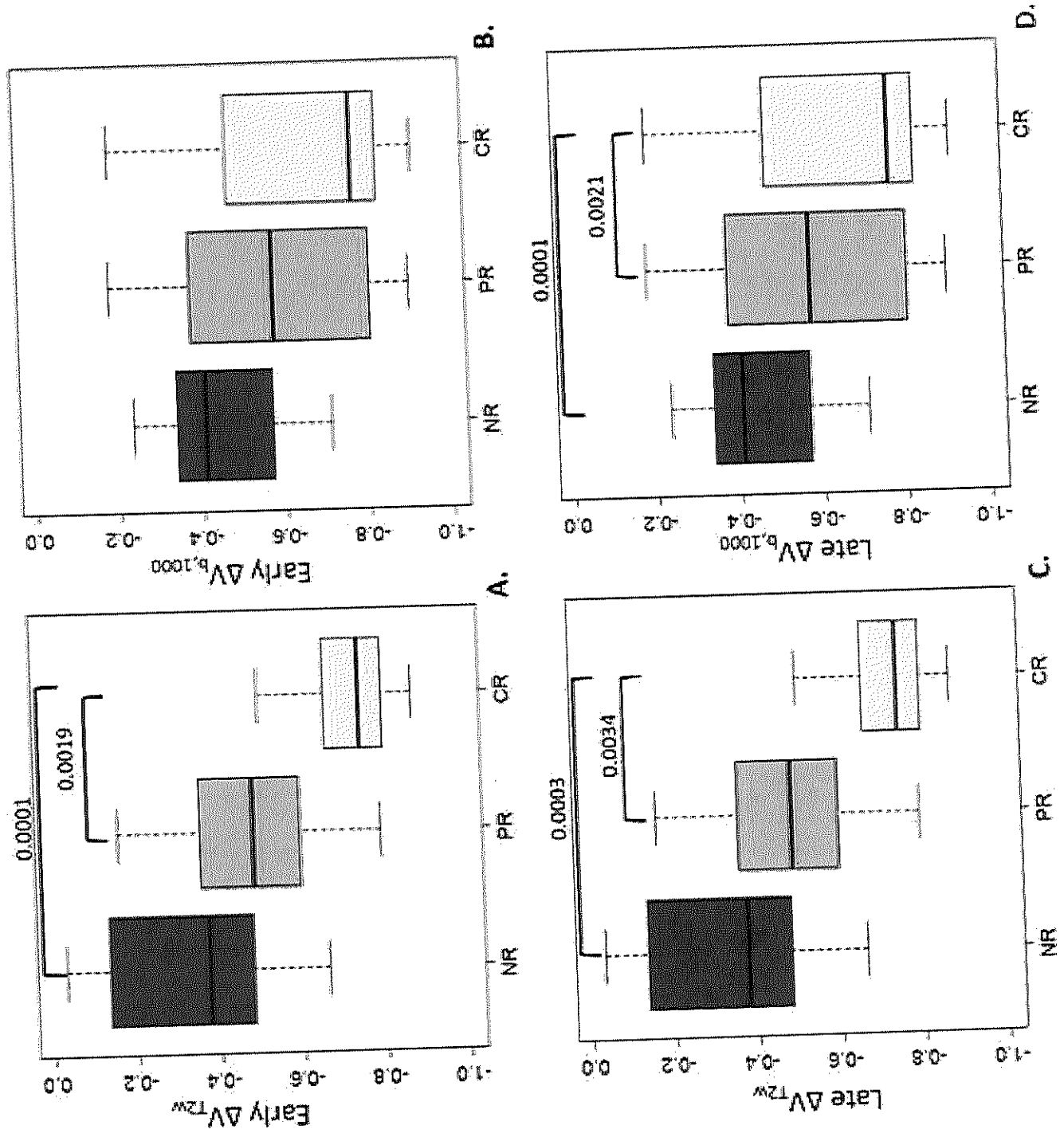
420 **Figure 5: ADC values according to TRG at each time point.** ADC values were significantly higher
421 in CR than PR and NR at pre-MRI (A), while resulted not significant different at mid (B) and post-MRI
422 (C). ADC values increased at mid-MRI (D, E, F), reaching statistical significance in NR and PR. ADC
423 at post-MRI was higher than at pre-MRI, with statistical significance in NR and PR.

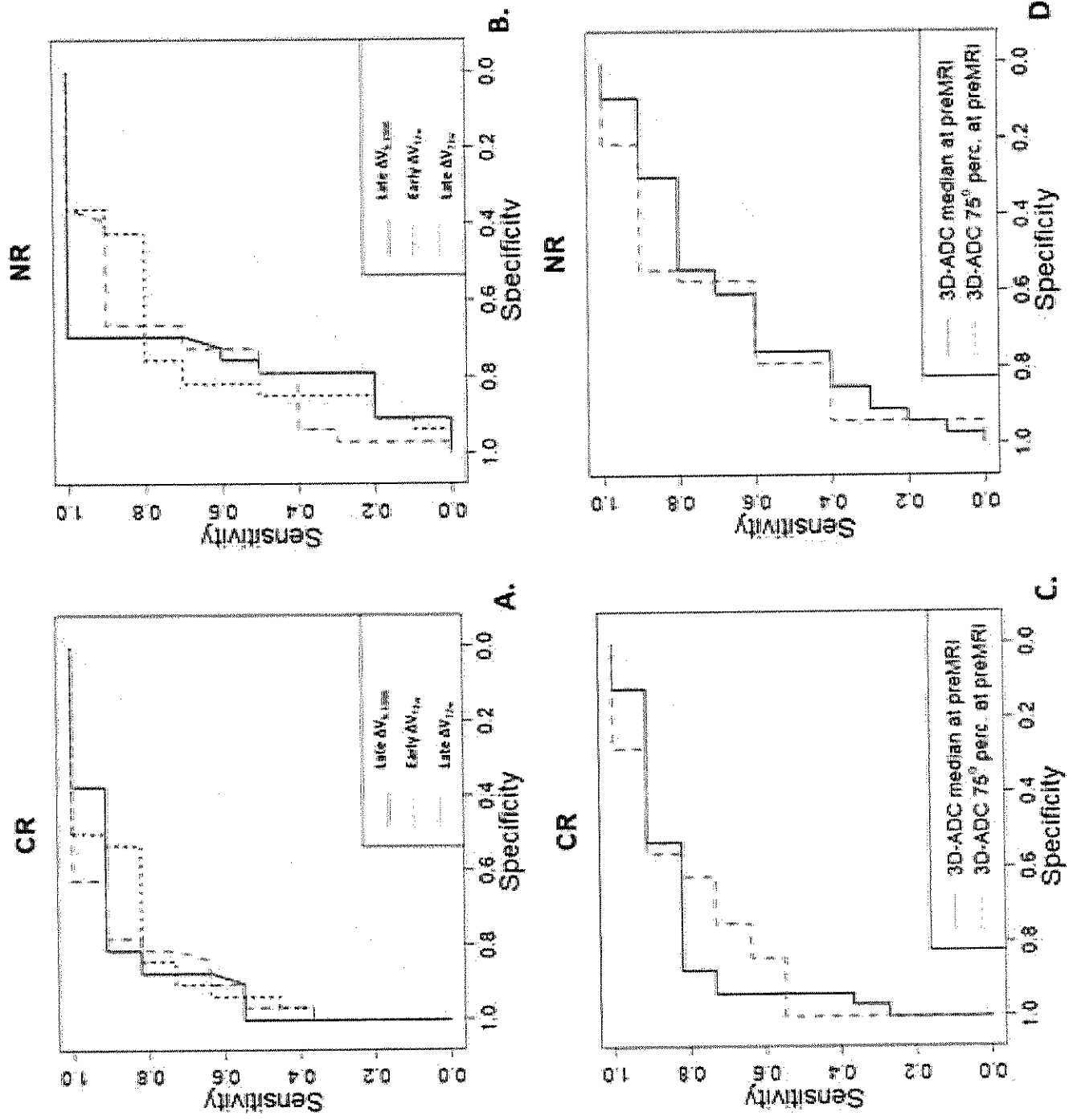
424

Revised Figure 1



Revised Figure 3





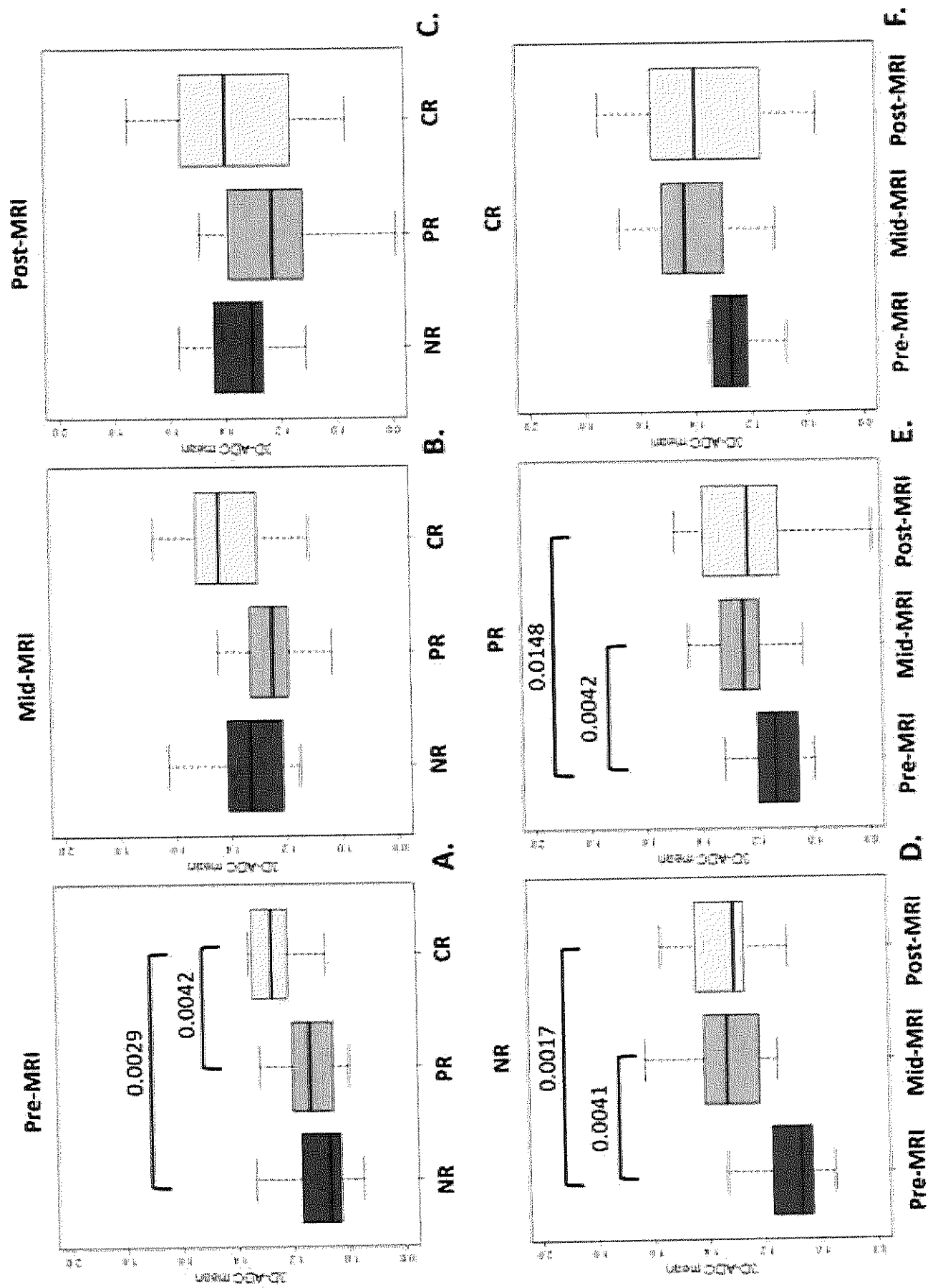


Table 1. Population features

Gender, n (%)	
Male	27 (63)
Female	16 (37)
Age, median(range, years)	61 (43-82)
Tumor location, n (%)	
Distal rectum	23 (53.5)
Middle rectum	11 (25.6)
Proximal rectum	9 (20.9)
Operative procedure, n (%)	
Low anterior resection	31 (72.1)
Ultra-low anterior resection	6 (13.9)
Intersphincteric resection	2 (4.7)
Abdominoperineal resection	4 (9.3)
Clinical T stage preCRT, n (%)	
2	4 (9.3)
3	33 (76.8)
4	6 (13.9)
Clinical N stage preCRT, n (%)	
N0	2 (4.7)
N+	41 (95.3)
pT Classification, n (%)	
0	11 (25.6)
1	4 (9.3)
2	10(23.2)
3	18 (41.9)
pN Classification, n (%)	
0	35 (81.4)
1 or 2	8 (18.6)
pTNM stage, n (%)	
0	11 (25.6)
I	12(27.9)
II	12 (27.9)
III	8 (18.6)

Table 2. Tumour volumes on T2w images (V_{T2w}) and DWI ($V_{b,1000}$) at each time point, with corresponding ΔV during (early ΔV) and post CRT (late ΔV) in relation to pathological response.

Tumour volumes results not significantly different among classes of pathological response at pre-MRI. They differed in term of V_{T2w} at mid-MRI, and in both V_{T2w} and $V_{b,1000}$ at post-MRI. Tumour volume reduction rate (ΔV) was different with respect to response so just during treatment if measured on T2w images, and after treatment at both the evaluation.

		NR	PR	CR	Adjusted p-value of Kruskal-Wallis' test
Pre-MRI	V_{T2w}	39.55 [23.02;62.8]	21.15 [16.71;38.26]	15.89 [11.75;35.98]	1.0000
	$V_{b,1000}$	43.74 [24.59;55.34]	21.73 [13.46;34.27]	12 [10.23;29.02]	0.6576
Mid-MRI	V_{T2w}	23.85 [11.83;40.82]	11.2 [7.7;19.93]	4.8 [2.35;9.6]	0.0400
	$V_{b,1000}$	23.29 [12.23;32.54]	8.94 [4.79;12.84]	5.12 [2.15;7.37]	0.0842
Post-MRI	V_{T2w}	12.04 [5.64;26.89]	6.39 [3.37;9.02]	2.4 [1.25;4.85]	0.0411
	$V_{b,1000}$	13.65 [9.54;15.86]	4.41 [2.42;7.55]	0.3 [0;1.85]	0.0026
Early (from pre-to-during CRT)	ΔV_{T2w}	-38% [-46%;-15%]	-49% [-59%;-36%]	-75% [-80%;-66%]	0.0020
	$\Delta V_{b,1000}$	-41% [-54%;-35%]	-58% [-80%;-39%]	-77% [-83%;-47%]	1.0000
Late (from pre-to-post CRT)	ΔV_{T2w}	-59% [-67%;-55%]	-75% [-79%;-60%]	-86% [-90%;-84%]	0.0050
	$\Delta V_{b,1000}$	-69% [-74%;-59%]	-78% [-88%;-56%]	-97% [-100%;-92%]	0.0020

Values are reported as median [Interquartile Range]

P-values of Kruskal-Wallis's test adjusted with Bonferroni's correction for each class of response are reported in Figure 1.

Table 3 Univariate multinomial regression for the prediction of the three classes of responders

	MRI Parameter	coefficient	adjusted p-value
Pre-MRI	VT2w	-0.0099	1.0000
	Vb, 1000	-0.0150	1.0000
	ADC mean	8.5552	0.0568
	ADC 25 ^o percentile	5.7735	0.3425
	ADC 75 ^o percentile	7.9213	0.0247
	ADC median	8.0007	0.0415
	ADC kurtosis	-0.5579	1.0000
	ADC skewness	-2.2652	0.1196
Mid-MRI	VT2w	-0.0182	1.0000
	Vb,1000	-0.0244	1.0000
	ADC mean	1.6645	1.0000
	ADC 25 ^o percentile	2.6341	1.0000
	ADC 75 ^o percentile	1.0303	1.0000
	ADC median	1.5337	1.0000
	ADC kurtosis	-0.4640	1.0000
	ADC skewness	-0.9912	1.0000
	Early ΔV_{T2w}	-6.4126	0.0028
	Early $\Delta V_{b,1000}$	-2.7576	0.4242
Post-MRI	VT2w	-0.0317	1.0000
	Vb,1000	-0.1214	0.1579
	ADC mean	0.1682	1.0000
	ADC 25 ^o percentile	2.6341	1.0000
	ADC 75 ^o percentile	1.0303	1.0000
	ADC median	1.5337	1.0000
	ADC kurtosis	-0.4640	1.0000
	ADC skewness	-0.9912	1.0000
	Late ΔV_{T2w}	-8.3833	0.0090
	Late $\Delta V_{b,1000}$	-5.4531	0.0265

In boldface p value <0.05.

Table 4. ROC analysis for prediction of either NR or CR by volumetric and 3D-ADC parameters significant at multinomial analysis.

Volumetric variables	Prediction of NR						Prediction of CR					
	AUC analysis		Best cut-off				AUC analysis		Best cut-off			
	Value	p-value	Value	Sensitivity	Specificity	Accuracy	Value	p-value	Value	Sensitivity	Specificity	Accuracy
Late $\Delta V_{b,1000}$	0.7742	0.0096	-77.3%	100%	70%	77%	0.8935	0.0001	-86.8%	91%	81%	84%
Early ΔV_{T2w}	0.7803	0.0082	-50.1%	90%	67%	73%	0.8991	0.0001	-58.3%	91%	78%	81%
Late ΔV_{T2w}	0.7576	0.0151	-69.1%	80%	76%	77%	0.8750	0.0003	-82.8%	82%	84%	84%
Pre-MRI 3D-ADC median	0.6727	0.1043	1.0245	60%	76%	72%	0.8409	0.0009	1.198	82%	88%	
Pre-MRI 3D-ADC 75 ^o perc	0.7242	0.0346	1.2835	60%	79%	74%	0.8239	0.0016	1.401	73%	75%	74%

Declaration of interests

The authors declare that they have no known competing financial interests or personal relationships that could have appeared to influence the work reported in this paper.

The authors declare the following financial interests/personal relationships which may be considered as potential competing interests:

Highlights:

- ADC histogram analysis may provide a new insight in pre-treatment rectal cancer evaluation.
- Tumour volume reduction rate from pre-to-during treatment is an early and accurate predictor of response to CRT.
- DWI are more sensitive than T2w images in the identification of residual tumour after treatment.

Please wait...

If this message is not eventually replaced by the proper contents of the document, your PDF viewer may not be able to display this type of document.

You can upgrade to the latest version of Adobe Reader for Windows®, Mac, or Linux® by visiting http://www.adobe.com/go/reader_download.

For more assistance with Adobe Reader visit <http://www.adobe.com/go/acrreader>.

Windows is either a registered trademark or a trademark of Microsoft Corporation in the United States and/or other countries. Mac is a trademark of Apple Inc., registered in the United States and other countries. Linux is the registered trademark of Linus Torvalds in the U.S. and other countries.

Please wait...

If this message is not eventually replaced by the proper contents of the document, your PDF viewer may not be able to display this type of document.

You can upgrade to the latest version of Adobe Reader for Windows®, Mac, or Linux® by visiting http://www.adobe.com/go/reader_download.

For more assistance with Adobe Reader visit <http://www.adobe.com/go/acrreader>.

Windows is either a registered trademark or a trademark of Microsoft Corporation in the United States and/or other countries. Mac is a trademark of Apple Inc., registered in the United States and other countries. Linux is the registered trademark of Linus Torvalds in the U.S. and other countries.